

SYNTHESIS OF NANOCRYSTALLINE BARIUM-HEXA FERRITE FROM  
NANOCRYSTALLINE GOETHITE USING THE HYDROTHERMAL METHOD:  
PARTICLE SIZE EVOLUTION AND MAGNETIC PROPERTIES

CONF-970481--1

R.L. Penn\*, J.F. Banfield\*\*, J. Voigt\*\*\*

\*Materials Science Program, University of WI - Madison, Madison, WI, 53706

rlee@geology.wisc.edu

\*\*Department of Geology and Geophysics, University of WI - Madison, Madison, WI, 53706

\*\*\*Ceramic Synthesis and Inorganic Chemistry Department, Sandia National Laboratories, Albuquerque, NM, 87185

RECEIVED

ABSTRACT

MAR 17 1997

To characterize particle size/magnetic property relationships, 9 to 50 nm in diameter barium hexaferite,  $\text{BaFe}_{12}\text{O}_{19}$  (BHF), particles were prepared using a new synthesis route. By replacing the conventional 50 to 100 nm particles of goethite with nanocrystalline goethite produced via the microwave anneal method of Knight and Sylva [1], nanocrystalline BHF was synthesized using the hydrothermal method. Evolution of particle size and morphology with respect to concentration and heat treatment time is reported. Hysteresis properties, including coercivity (0.2 - 1.0 kOe), magnetization saturation (0.1-33.4 emu/g), and magnetization remanence (0.004 - 22.5 emu/g) are discussed as a function of particle size. The magnetization saturation and remanence of the 7 nm particles is nearly zero, suggesting the superparamagnetic threshold size for BHF is around this size. In addition, the equilibrium morphology of BHF crystals was calculated to be truncated hexagonal prisms which was verified by experiment, and the isoelectric point, pH of 4.1, was measured for 18 nm BHF particles.

INTRODUCTION

MASTER

The hexagonal ferrites, a group of ferromagnetic oxides, are important because of their high coercive force [2]. The synthesis and characterization of M-type barium hexaferite,  $\text{BaFe}_{12}\text{O}_{19}$  (BHF), has received much attention recently because of its potential for use in high density magnetic storage systems and permanent magnets [3-7]. For example, the bit size of magnetic recording could be reduced through a compromise between optimizing BHF magnetic properties and reducing particle size. Theoretically, the superparamagnetic threshold size for BHF could be less than 10 nm [8]. In addition, this material is chemically inert, has high magnetic anisotropy, is mechanically hard, and exhibits compositional flexibility which can result in modification of magnetic properties [9]. Thus, understanding the connection between the preparation technique, morphology, and magnetic properties is essential [3,5].

The hydrothermal method of synthesizing oxides has recently become an important technique because of its low temperature requirements, high quality particle production, and elimination of the final high temperature calcination step common to many oxide syntheses. Several examples of the hydrothermal synthesis of BHF exist in the literature [10-17]. These syntheses, involving autoclaving of a suspension of goethite or hematite and barium hydroxide, produce BHF particles typically in the micron range. This paper presents a new method of synthesizing nanocrystalline BHF particles using a nanocrystalline goethite precursor via the hydrothermal synthesis route, reports particle size control, and the relationship between particle size and hysteresis properties.

EXPERIMENT

DISTRIBUTION OF THIS DOCUMENT IS UNLIMITED

Following the method of Knight and Sylva [1], a sol of 3-5 nm goethite particles (nano-g) was synthesized. Solutions of 0.238 M sodium bicarbonate and 0.200 M ferric nitrate were filtered using 0.2  $\mu\text{m}$  filter membrane. The sodium bicarbonate solution was added drop wise to the vigorously stirred ferric nitrate solution over a period of 45 minutes.

#### **DISCLAIMER**

**Portions of this document may be illegible  
in electronic image products. Images are  
produced from the best available original  
document.**

This mixture was allowed to stir for one hour before microwave annealing at high power in a standard microwave for four periods of about 40 seconds with shaking between each period. The suspension had just begun to boil at the end of the fourth period. The resulting suspension was immediately placed in an ice bath, and then placed in a Spectra Por dialysis bag (MWCO = 2000 g/mol), which was placed in a container of DI water. This water was changed four times over a period of 48 hours. HRTEM revealed the particles were slightly acicular, aspect ratio ~1.5, and were 3-5 nm long, as shown in figure 1. No particles larger than 6 nm were observed.

Suspensions of nano-g (0.025 M  $\text{Fe}^{+3}$ ) and barium hydroxide (0.025 M  $\text{Ba}^{+2}$ ) were prepared (pH = 12.4) and placed in Teflon lined steel bombs (Parr Instruments # 4744). The bombs were then placed in a furnace heated to 250°C for two and five hours. Suspensions twice as concentrated (pH = 12.6) were treated in the same manner for two, four, and eight hours. Suspensions of 0.05 M nano-g and barium hydroxide, adjusted to a pH of 13.1 using sodium hydroxide, were prepared and heat treated at 250°C for two, four, eight, 24, and 48 hours.

The molar ratio of barium hydroxide to goethite was varied while maintaining a constant goethite concentration. Ratios of 0.5, 0.75, and 1.0 and goethite concentrations of 0.047M and 0.023M were used. Preparation technique was identical to that described above, and the heat treatment temperature was 250°C.

Resulting powders were X-rayed using a Scintag powder diffractometer and examined using the Philips CM200UT Transmission Electron Microscope (TEM) equipped with an Energy Dispersive X-ray (EDX) detector. Average particle size and aspect ratio were determined from TEM images. Magnetic measurements were performed at the Institute for Rock Magnetics in Minneapolis, MN using an alternating gradient force magnetometer.

Electrophoretic mobilities of five suspensions of 18 nm BHF particles prepared at pH's of 3.3, 4.6, 7.2, 9.0, and 10.4 were measured using the Pen Kem System 3000 in order to determine the isoelectric point. The pH's were adjusted by adding acetic acid or ammonium hydroxide to the suspensions, and pH's were remeasured after the suspensions were allowed to stand for 24 hours.

## RESULTS AND DISCUSSION

Heat treatment at 250°C of 0.025 M barium hydroxide and 0.025 M  $\text{Fe}^{+3}$  (from nano-g sol) resulted in BHF particle growth. Formation of BHF was confirmed using X-ray diffraction (XRD) to verify structure and EDX to verify composition. XRD results show the main products to be BHF and witherite ( $\text{BaCO}_3$ ). In addition, a small amount of hematite,  $\text{Fe}_2\text{O}_3$ , is sometimes produced. Based on TEM data, after two hours the

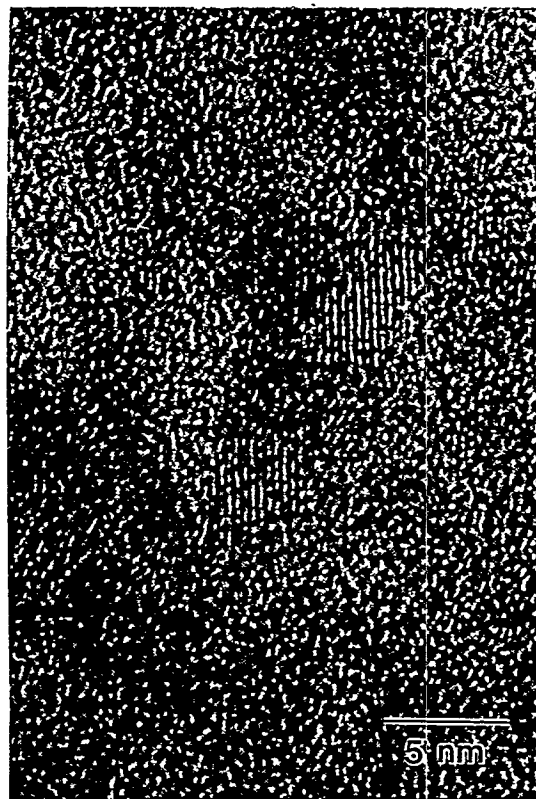


Figure 1: TEM micrograph of goethite particles produced using Knight and Sylva's microwave anneal method.

average BHF particle size was 9 nm; after five hours, 18 nm; and after 45 hours, 21 nm. The particle size distribution profile, which is typical of all trials, for 9 nm BHF particles is shown in figure 2, and the evolution of particle size is shown in figure 3. BHF particles were rounded and slightly elongated perpendicular to the  $c$ -axis. No clear expression of crystallographic faces was observed (figure 4). For comparison, figure 5 shows typical micron sized BHF particles obtained using the same synthesis conditions as above, but using 50-100 nm goethite starting material. Different heat treatment times and temperatures do not result in particle growth, and expression of the truncated hexagonal prism morphology is clearly observed.

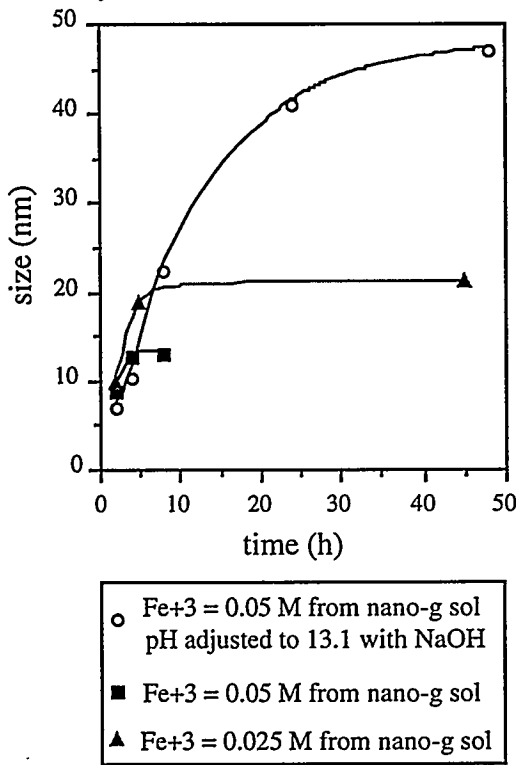


Figure 3: Evolution of particle size with respect to time. Suspensions were prepared and placed in a 250°C furnace for various times.  $\text{Ba}^{+2} : \text{Fe}^{+3}$  ratio is equal to one in all cases.

Doubling the concentration of barium hydroxide and nano-g resulted in slower particle growth. Heat treatment at 250°C for two, four, and eight hours resulted in average BHF particles sizes of 8.6, 12.5, and 13.1 nm respectively, as shown in figure 3. These particles exhibited the same elongation perpendicular to the  $c$ -axis and rounded appearance as the first set of experiments.

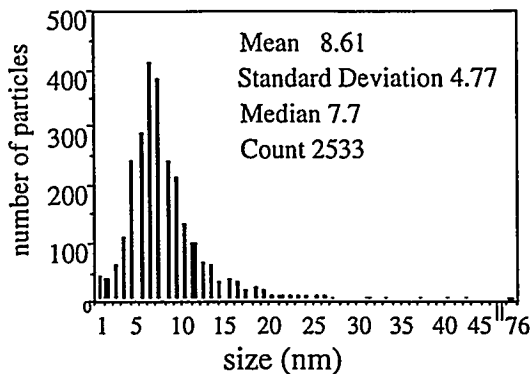


Figure 2: Typical particle size distribution for BHF particles produced in this study. Synthesis conditions for this sample were 0.025 M  $\text{Fe}^{+3}$  (from nano-g) and 0.025 M  $\text{Ba}(\text{OH})_2$  suspension heat treated at 250°C for two hours.

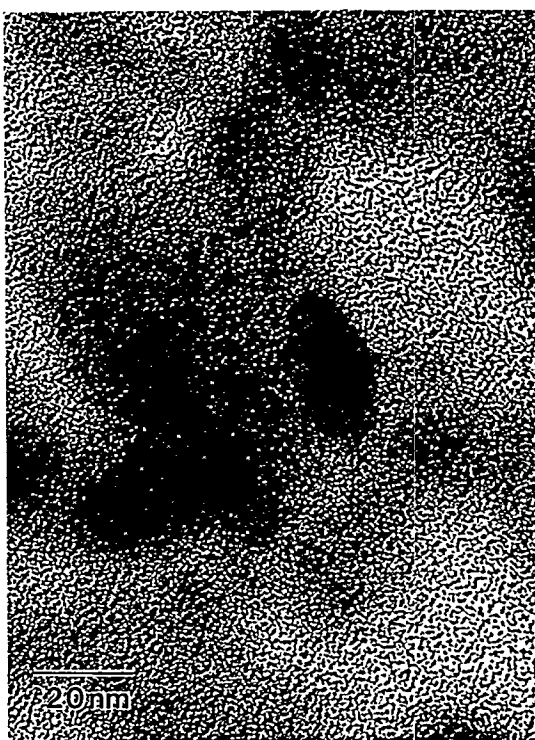


Figure 4: TEM micrograph of nanocrystalline BHF particles (average particle size = 8.6 nm). These particles were produced from a 0.025M  $\text{Fe}^{+3}$  (from nano-g precursor) and 0.025 M  $\text{Ba}(\text{OH})_2$  suspension heat treated at 250°C for two hours.

Increasing the pH of the starting suspension using sodium hydroxide resulted in enhanced growth of BHF particles. Particle size evolution with respect to time is shown in figure 3. The initial growth rate is similar to previous trials, but the growth of intermediate sized particles and the size at which growth levels off are strongly enhanced in the NaOH modified suspensions.

Figure 3 shows the particle size evolution of all particles produced in this study. Initial BHF particles are similar in size to the starting nano-g particles, suggesting a topotactic transformation from goethite to BHF. Rapid acceleration of particle growth is observed between two and four hours, with substantial slowing after four hours in all three sets. Doubling the concentration of goethite and barium hydroxide resulted in a significantly slower growth rate of intermediate sized particles and a smaller particle size at which the growth rate levels off. Increase of the pH of the goethite and barium hydroxide suspension resulted in enhanced particle growth with significant extension of the size range over which significant particle growth is observed. This could reflect increased solubility of species present during growth.

Experiments following the above pH, concentration, and molar ratio variations using 50-100 nm goethite as the iron source never resulted in the production of nanocrystalline BHF. However, production of nanocrystalline BHF when the starting iron source was nano-g suggests a topotactic transformation mechanism for BHF formation, followed by dissolution of smaller particles and reprecipitation onto larger particles. At higher pH, the growth mechanism of dissolution and reprecipitation was most likely enhanced due to higher solubility of species present, resulting in faster growth of BHF particles.

Varying the molar ratio of barium hydroxide to  $\text{Fe}^{+3}$  concentration showed that the most efficient BHF production is attained at a molar ratio of one. Qualitative comparison of peak intensities between trials shows that less hematite, less witherite, and more BHF is produced at a molar ratio of one than at lower molar ratios.

In addition, pH adjustment of suspensions using NaOH results in less efficient BHF production. XRD results indicate higher production of witherite, and lower production of BHF. No sodium contamination of BHF particles was observed in EDX results. Figure 6 shows the evolution of particle size and aspect ratio with respect to time. For particles with diameters under 24 nm, the same elongation and rounded appearance as in previous trials was observed. However, the 41 and 47 nm particles showed expression of the hexagonal tablet morphology (figure 7).

Qualitative analysis of XRD data show more efficient production of BHF with a heat treatment temperature of 250°C at all time periods. 250°C heat treatment results show witherite and hematite production to be significantly less than the lower heat treatment temperatures of 190°C, 210°C, and 230°C used. At 250°C, BHF begins to form after two hours; 230°C, after four hours; 210°C, after seven hours; and 190°C, after 24 hours. In addition, the increase of suspension pH using sodium hydroxide resulted in more witherite production, but no hematite or goethite was observed in the final powders.



Figure 5: TEM micrograph of micron sized BHF particles. These particles were produced from a 0.025M  $\text{Fe}^{+3}$  (from 50-100 nm goethite precursor) and 0.025 M  $\text{Ba}(\text{OH})_2$  suspension heat treated at 250°C for eight hours. The hexagonal face is {001}.

Hysteresis properties were measured for the resulting materials. Figure 8 plots the saturation and remanent magnetizations versus particle size, and figure 9 plots the coercivity versus particle size. As predicted by theory, the saturation and remanent

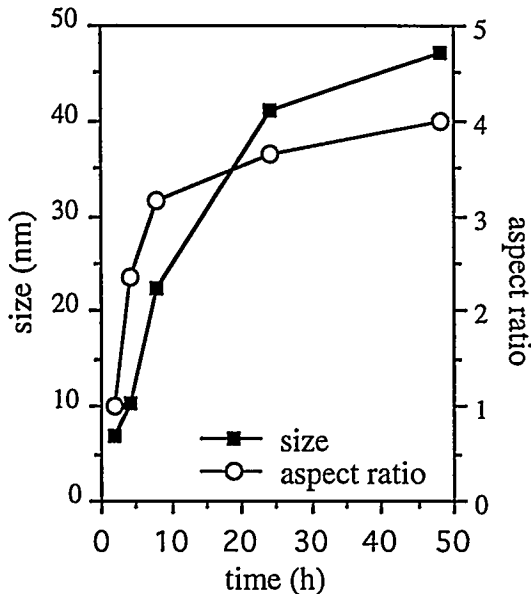


Figure 6: Evolution of particle size and aspect ratio with respect to heat treatment (250°C) time. Particle size data is also included in figure 3. The starting suspensions were 0.05 M  $\text{Fe}^{+3}$  (from nano-g sol) and 0.05 M  $\text{Ba}(\text{OH})_2$  adjusted to a pH of 13.1 using sodium hydroxide. These were then placed into a 250°C furnace for various times.



Figure 7: TEM micrograph of BHF particles produced from 0.05 M  $\text{Fe}^{+3}$  (from nano-g sol) and 0.05 M  $\text{Ba}(\text{OH})_2$  suspension placed in a 250°C furnace for 48 hours.

magnetizations and the coercivity increase with increasing particle size up to the limiting single domain size [18]. In addition, the magnetization saturation and remanence of the 6.8 nm particles is nearly zero, suggesting the superparamagnetic threshold size for BHF is around this size. This is consistent with the theoretical prediction [8].

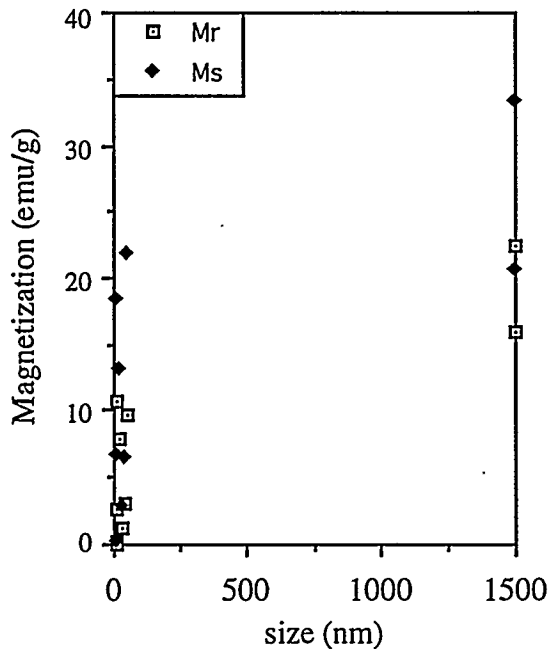


Figure 8: Remanent and Saturation magnetization versus BHF particle size.

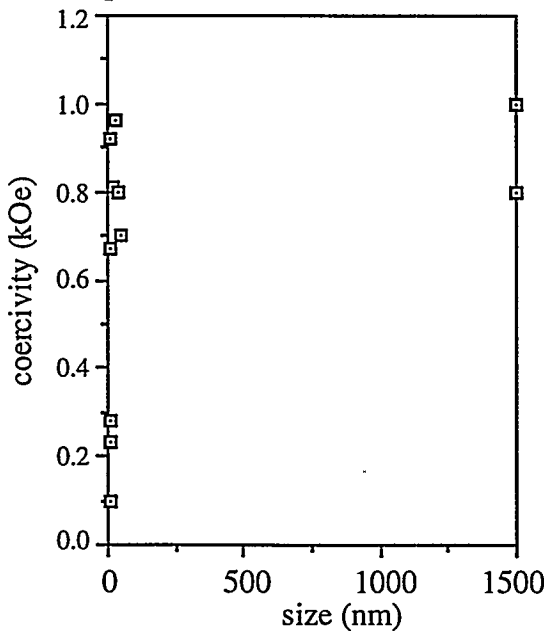


Figure 9: Coercivity versus BHF particle size.

The equilibrium morphology of BHF was calculated to be truncated hexagonal prisms using the Catalysis program from Biosym/MSI of San Diego. In particular, this calculation used the Donnay Harker rules, which relate surface energy to the interplanar spacing. The dominant observed (figure 5) and calculated crystallographic face is the {001}, which corresponds to the largest  $d_{hkl}$ . Crystal morphology is controlled by the slowest growing face [19], which means that particle morphology can be modified if the surface energy or growth rate of a particular family of crystallographic faces can be changed. Calculating the morphology after increasing the surface energy, or increasing the growth rate, of the {001} type face results in long thin acicular crystals with {100} as the dominant face. Crystallographically specific adsorption may result in such morphology modification. This will be the focus of future experimental and computer modeling studies.

Plotting the mobilities of the 18 nm BHF particles versus pH of the suspension shows that the isoelectric point is about 4.1 (figure 10). Characterization of the surface chemistry of BHF particles will be important in adsorption-route morphology modification studies.

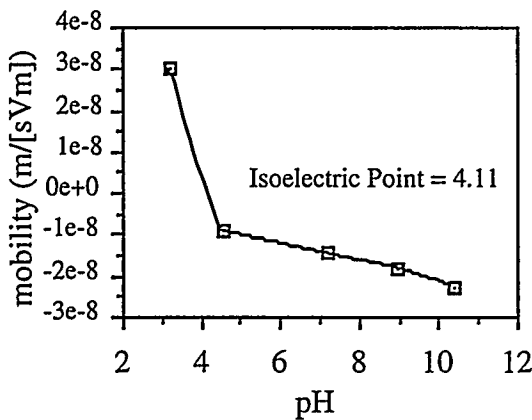


Figure 10: Electrophoretic mobilities versus pH of 18 nm BHF suspensions.

## CONCLUSIONS

This paper reports a new route for production of nanocrystalline BHF particles using a nanocrystalline goethite precursor and control of BHF particle size with respect to heat treatment time, concentration of precursors, and an increase in pH. In addition, hysteresis and surface properties are reported. Hysteresis properties were observed to increase with increasing particle size. The saturation and remanent magnetization of the 7 nm BHF particles nearly zero, suggesting the superparamagnetic threshold size for BHF is around this size.

## REFERENCES

1. R. Knight and R. Sylva, *J. Inorg. Nucl. Chem.*, **36**, 591-597 (1974).
2. W. Townes, J. Fang, and A. Perrotta, *Z. Kristallogr.*, **125**, 437-449 (1967).
3. M. El-Hilo, H. Pfeiffer, K. O'Grady, W. Schüppel, E. Sinn, P. Görnert, M. Rösler, D. Dickson, and R. Chantrell, *J. Magn. Magn. Mater.*, **129**, 339-347 (1994).
4. K. Higuchi, S. Hirano, and S. Naka, *Int'l. Conf. on Ferrites* (4th : 1984 : San Fransiciso, CA), *Adv. Ceram.*, **15-16**, 73-79 (1984).
5. K. Higuchi, S. Naka, and S. Hirano, *Adv. Ceram. Mater.*, **3**, 278-281 (1988).
6. Z. Tang, S. Nafis, C. Sorensen, and G. Hadjipanayis, *IEEE Trans. Magn.*, **25**, 4236-4238 (1989).
7. M. Sharrock, *IEEE Trans. Magn.*, **26**, 225-227 (1990).
8. V. Sankaranarayanan, Q. Pankhurst, D. Kickson, and C. Johnson, *J. Magn. Magn. Mater.*, **125**, 199-208 (1993).

9. R. Atkinson, P. Papakonstantinon, I. Salter, R. Gerber, *J. Magn. Magn. Mater.*, **138**, 222-231 (1994)
10. D. Barb, L. Diamandescu, A. Rusi, D. Tarabasanu-Mihaila, M. Morariu, V. Teodorescu, *J. Mat. Sci.*, **21**, 1118-1122 (1986).
11. C. Lin, Z. Shih, T. Chin, M. Wang, and Y. Yu, *IEEE Trans. Magn.*, **26**, 15-17 (1990).
12. M. Wang, Z. Shih, and C. Lin, *Ind. Eng. Chem. Res.*, **31**, 828-833 (1992a).
13. M. Wang, Z. Shih, and C. Lin, *J. Cryst. Growth*, **116**, 483-494 (1992b).
14. M. Wang and Z. Shih, *J. Cryst. Growth*, **114**, 435-445 (1991).
15. M. Wang, Z. Shih, and C. Lin, *Chem. Eng. Comm.*, **126**, 79-95 (1993a).
16. M. Wang, Z. Shih, and C. Lin, *J. Cryst. Growth*, **130**, 153-161 (1993b).
17. S. Komarneni, E. Fregeau, E. Breval, and R. Roy, *J. Am. Ceram. Soc.*, **71**, C-26 - C-28 (1988).
18. B. Cullity, *Introduction to Magnetic Materials*, Reading, Addison-Wesley, 1972.
19. J. Mullin, *Crystallization*, London, Butterworths, 1961.

#### ACKNOWLEDGEMENTS

This research received support from NSF grant EAR - 9508171, subcontract 144 - ED81 from Sandia National Laboratories, and a scholarship from the National Physical Science Consortium to R. Lee. Penn.

This work was supported by the United States  
Department of Energy under Contract  
DE-AC04-94AL 85000.  
Sandia is a multiprogram laboratory operated by  
Sandia Corporation, a Lockheed Martin Company,  
for the United States Department of Energy.

#### DISCLAIMER

This report was prepared as an account of work sponsored by an agency of the United States Government. Neither the United States Government nor any agency thereof, nor any of their employees, makes any warranty, express or implied, or assumes any legal liability or responsibility for the accuracy, completeness, or usefulness of any information, apparatus, product, or process disclosed, or represents that its use would not infringe privately owned rights. Reference herein to any specific commercial product, process, or service by trade name, trademark, manufacturer, or otherwise does not necessarily constitute or imply its endorsement, recommendation, or favoring by the United States Government or any agency thereof. The views and opinions of authors expressed herein do not necessarily state or reflect those of the United States Government or any agency thereof.